Can the Drake Passage affect the ENSO variability?

Zhanghanshu Han[a], Haijun Yang*[a], Mingjun Tong[a], Peixi Wang[b], Xiaoming Hu[b], and Song Yang[b]

[a] *Department of Atmospheric and Oceanic Sciences, Institute of Atmospheric Sciences, and Key Laboratory of Polar Atmosphere-ocean-ice System for Weather and Climate of Ministry of Education, Fudan University, Shanghai 200438, China*

[b] *School of Atmospheric Sciences, Sun Yat-sen University and Southern Marine Science and Engineering Guangdong Laboratory (Zhuhai), Zhuhai 519082, China*

Ocean-Land-Atmosphere Research

April 5, 2026

Submitted

**Corresponding author*: Haijun Yang, yanghj@fudan.edu.cn

ABSTRACT

This study investigates the role of the opening of the Drake Passage (DP) in El Niño–Southern Oscillation (ENSO) variability using fully coupled model experiments with the DP closed (DPC) and open (DPO). The opening of the DP leads to the establishment of the Antarctic Circumpolar Current and strengthening of the Atlantic Meridional Overturning Circulation, warming the Northern Hemisphere and cooling the Southern Hemisphere. This causes the southern branch of the Hadley cell to shift northward and intensify, strengthens the Southern Hemisphere trade winds, and leads to more warm water accumulation in the equatorial Pacific, an enhanced meridional temperature gradient between the equator and the Southern Hemisphere. Through analysis of the terms in the temperature variance equation, the stronger anomalous upwelling is the primary cause of the enhanced ENSO variability. The enhanced meridional temperature gradient increases the zonal wind stress variability, which in turn strengthens anomalous upwelling. Our findings imply that the influence of DP opening on tropical climate variability has been previously underestimated.

KEYWORDS: Drake Passage; paleoclimate; ENSO; tropical Pacific; CESM

1. Introduction

The Drake Passage (DP), located between Cape Horn at the southern tip of South America and the South Shetland Islands in Antarctica, is the widest and deepest strait on Earth and plays a key regulatory role in the global climate system (Toggweiler & Samuels, 1995; Toggweiler & Bjornsson, 2000; Sijp & England, 2004, 2005; Sijp et al., 2009; Zhang et al., 2010, 2011; Yang et al., 2014; Wang et al., 2024, 2025). It connects the Pacific and Atlantic Oceans, enabling the direct exchange of heat and salinity between the two largest basins (Chidichimo et al., 2014; Koenig et al., 2014; Donohue et al., 2016; Gutierrez-Villanueva et al., 2023; Song et al., 2025; Xie et al., 2025). Owing to its location within the westerly wind belt, combined with its broad expanse and the absence of land barriers, the DP provides essential conditions for the existence of a vigorous Antarctic Circumpolar Current (ACC) (Sijp & England, 2004, 2005; Sijp et al., 2009; Zhang et al., 2010, 2011; Yang et al., 2014; Wang et al., 2024, 2025). Observations show that the ACC transport through the DP exceeds 140 Sv and remains remarkably stable over the past few decades (Chidichimo et al., 2014; Koenig et al., 2014; Donohue et al., 2016; Gutierrez-Villanueva et al., 2023).

Serving as the key Southern Ocean gateway, DP was fully closed until approximately 50 million years ago (Ma) and began to open around 30 Ma (Zachos et al., 2001; Lagabrielle et al., 2009). Modeling experiments investigating the closure, opening, and depth variations of the DP indicate that the establishment of the strong modern ACC only followed the opening of it. This reorganization reduced heat transport toward Antarctica, leading to Antarctic cooling and expanded sea ice coverage in the Southern Ocean, thereby creating profound differences in global ocean circulation and climate compared to the pre-opening configuration (Toggweiler & Samuels, 1995; Toggweiler & Bjornsson, 2000; Sijp & England, 2004, 2005; Sijp et al., 2009; Yang et al., 2014; England et al., 2017; Wang et al., 2024, 2025). Early studies primarily focused on how the tectonic configuration of DP influenced global climate through its impact on the ACC and Atlantic Meridional Overturning Circulation (AMOC) (Toggweiler & Samuels, 1995; Toggweiler & Bjornsson, 2000; Sijp & England, 2004, 2005; Sijp et al., 2009), and later work by Yang et al. (2014) expanded this perspective by incorporating the closure of the Panama Seaway into the discussion. Zhang et al. (2010, 2011) accounted for Cenozoic paleogeography and greenhouse gas concentrations in their investigations, while Wang et al. (2024, 2025) subsequently linked this issue to asymmetric polar warming.

Topographic features including straits and mountains (e.g., the Tibetan Plateau) represent a major condition that shapes climate and ocean circulation (Ruddiman & Kutzbach, 1989; Molnar et al., 1993; Kitoh, 1997; Yang et al., 2024; Tong et al., 2025) and thereby influence ENSO (Kitoh, 2006; Feng & Poulsen, 2014; Fallah et al., 2016; Naiman et al., 2017; Wen et al., 2020). In addition to the effects of atmospheric circulation changes induced by topographic forcing on tropical variability, the ocean meridional overturning circulation that transports extratropical signals into the tropics also plays a crucial role in the equatorial thermocline structure and stability (Liu & Yang, 2003; Yang et al., 2005; Zhang et al., 2005). Besides mountains, the evolution of oceanic gateways also plays a crucial role in shaping the climatic mean state (Zhang et al., 2011).

The El Niño–Southern Oscillation (ENSO) is the most prominent interannual variability in the tropical Pacific, representing a manifestation of ocean-atmosphere coupling (McPhaden et al., 2006). Its characteristics (e.g. amplitude, frequency, spatial pattern, and asymmetry) are fundamentally modulated by the background mean climate state of the tropical Pacific (Collins, 2000; Fedorov & Philander, 2001; Timmermann et al., 2018). Key mean-state parameters such as the strength of the trade winds, the zonal sea surface temperature (SST) gradient, the depth, stratification and vertical heat flux of the equatorial thermocline, and the stability of the ocean-atmosphere coupling collectively determine the variability and period of ENSO (Guilyardi, 2006; Jin et al., 2006; Kug et al., 2009; Sun et al., 2009; Chen et al., 2013; Wang et al., 2013; Liu et al., 2014). Paleoclimatic records indicate that ENSO has undergone significant shifts in response to past changes in boundary conditions, such as ice-sheet extent and orbital forcing (Tudhope et al., 2001; Cobb et al., 2003; Liu et al., 2014).

However, it remains a question whether the oceanic and atmospheric circulation adjustments induced by the opening of DP can influence low-latitude, tropical air-sea interaction processes, particularly the strongest mode of variability, ENSO. In this study, we investigate this question using the fully coupled Community Earth System Model (CESM) version 1.2.2 to conduct simulations with an open DP and a closed DP (see Section 2). By comparing the results from these two experiments, we investigate the impact of DP opening on tropical climate and ENSO.

The article is structured as follows. Section 2 describes the model and experimental design. Section 3 presents the changes in ENSO and the tropical Pacific mean climate between the topographic experiments. Section 4 analyzes the mechanisms underlying the changes in ENSO variability, followed by a summary and discussion in Section 5.

2. Model and Experiments

The fully coupled CESM used in this study is a global climate model (Hurrell et al., 2013). Its atmospheric component is the Community Atmosphere Model version 4 (CAM4) with a horizontal resolution of approximately 1.9° latitude by 2.5° longitude and 26 vertical layers in a hybrid sigma-pressure coordinate, extending to a model top at 35 km. The ocean and sea ice components have a nominal horizontal resolution of 1° with 60 vertical layers, reaching a maximum depth of 5.5 km. The atmospheric CO_2 concentration is prescribed at a year-2000 level of 367 ppm.

Two fully coupled experiments are conducted: a closed DP (DPC) and an open DP (DPO). In the DPC experiment, an isthmus approximately 500 km wide and 10 m high connects the Antarctic Peninsula to Cape Horn, South America (Sijp & England, 2004, 2005; Sijp et al., 2009; Yang et al., 2014). The DPO simulation was spun up for 249 years to reach a quasi-equilibrium state. For DPC, a longer spin-up of 900 years was required due to the extended adjustment timescale of the ocean circulation. The analysis in this study is based on a subsequent 100-year integration from each equilibrated state. More detailed experimental design and a model-observation comparison can be found in Wang et al. (2024, 2025).

3. Results

Figure 1 presents the time series of ENSO variability for both the DPC and DPO experiments. It displays the SST anomaly (SSTA) in the Niño-3.4 region (5°S–5°N, 150°E–90°W) from both experiments. In the DPO experiment, the standard deviation of SSTA (σ) is 0.92°C. In contrast, the DPC experiment exhibits weaker tropical SSTA oscillations, with σ reduced to approximately 0.52°C. Overall, ENSO variability is notably enhanced following the opening of the DP. To understand why ENSO variability in the tropical Pacific increases, it is necessary to first examine the changes in the climates of both hemispheres induced by the DP opening.

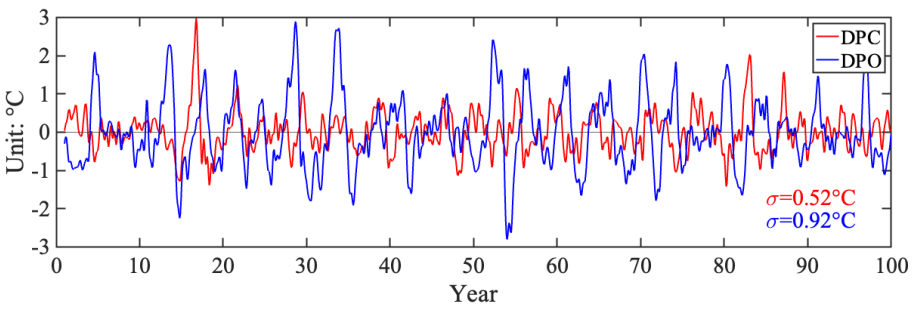

123 FIG. 1. Time series of SST anomalies (SSTA) and their standard deviation (σ) averaged over
124 the Niño-3.4 region (5°S–5°N, 150°E–90°W) are shown in the figure. The SSTA field is smoothed
125 with a 5–85-month bandpass filter.

126

127 In the modern climate, the AMOC constitutes the primary component of the global
128 meridional overturning circulation and dominates the northward cross-equatorial heat transport in
129 the Southern Hemisphere (Wen & Yang, 2020; Yang et al., 2024). The AMOC consists of both
130 thermohaline and wind-driven components (Weaver et al., 1993; Rahmstorf, 2002). Previous
131 modeling studies have demonstrated that the opening, closure, and depth of the DP have a strong
132 influence on the AMOC (Toggweiler & Samuels, 1995; Toggweiler & Bjornsson, 2000; Sijp &
133 England, 2004, 2005; Sijp et al., 2009; Yang et al., 2014; England et al., 2017). Among these, the
134 earliest studies even proposed that a closed DP would shut down the formation of a vigorous
135 AMOC. Using freshwater hosing experiments, Sijp and England (2005) identified a threshold
136 depth for the DP necessary to sustain an AMOC. Subsequent research using fully coupled models
137 found that, under modern continental configurations and greenhouse gas levels, a closed DP does
138 not completely halt the formation of North Atlantic Deep Water (NADW) and thus does not
139 entirely shut down the AMOC (Yang et al., 2014; England et al., 2017; Wang et al., 2024, 2025).

140 Figure 2 depicts the AMOC stream function in the DPC and DPO experiments. Under the
141 DPC configuration, the AMOC does not collapse due to NADW formation (Figure 2a). The
142 opening of the DP creates the necessary conditions for the development of a vigorous ACC. The
143 enhanced ACC strengthens the wind-driven Ekman pumping upwelling in the Southern Ocean
144 (Wang et al., 2024), constituting a key mechanism for returning deep waters to the surface. The
145 resulting northward Ekman divergence greatly strengthens the upper limb of the AMOC and
146 enhances northward heat transport (Toggweiler & Samuels, 1995; Sijp & England, 2004; Wang et
147 al., 2024).

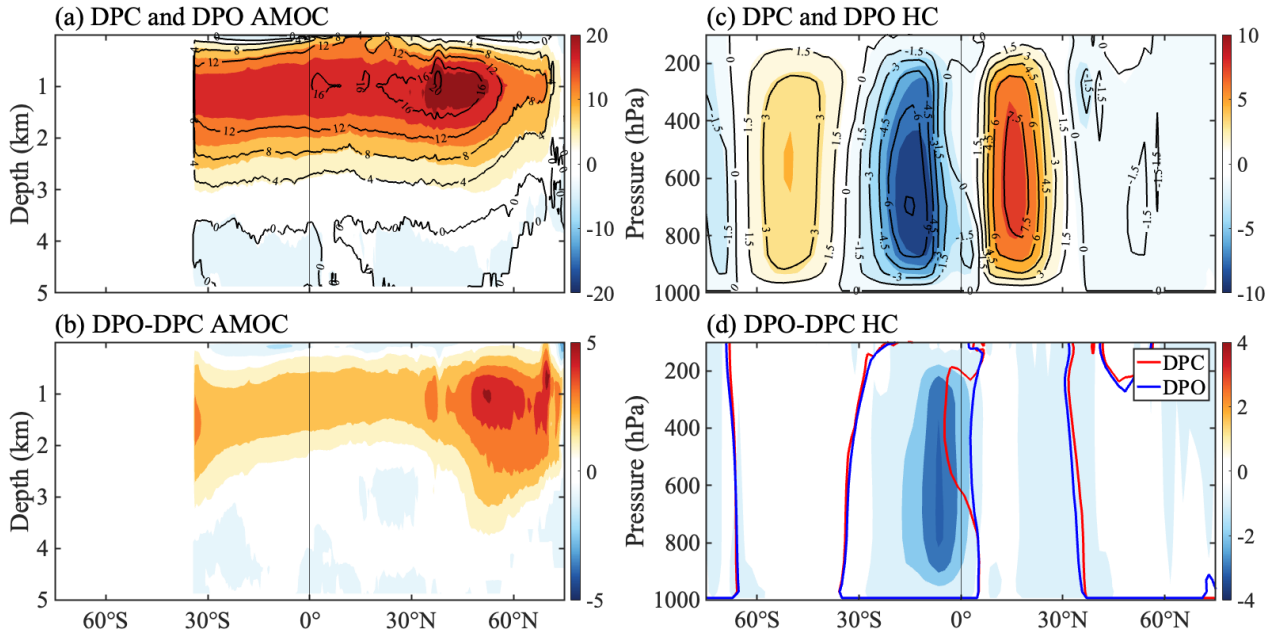

FIG. 2. Patterns of the AMOC stream function (Sv) in (a) contours for DPC and shading for DPO, and (b) DPO minus DPC. Mean Hadley cell (HC) stream function (10^{10} kg s^{-1}) in (c) contours for DPC and shading for DPO, and (d) DPO minus DPC. The red and blue lines in (d) indicate the zero stream function lines for DPC and DPO, respectively.

Due to the increased northward heat transport, the Northern Hemisphere becomes relatively warmer, causing the southern branch of the Hadley cell (HC) to shift northward and intensify. Notably, the boundary of the rising branch above 700 hPa moves from the Southern Hemisphere into the Northern Hemisphere (Figure 3d). Both model simulations and paleoclimate proxies demonstrate that when the AMOC strengthens, the enhanced northward heat transport warms the Northern Hemisphere, thereby driving the global HC and the Intertropical Convergence Zone (ITCZ) to shift northward toward the warmer hemisphere (Broccoli et al., 2006; Stouffer et al., 2006; Yang et al., 2014; Liu & Hu, 2015; McGee et al., 2018; Kug et al., 2021; Kim et al., 2023; Oh et al., 2024).

Meanwhile, the intensification of the HC explains the significantly enhanced northward latent energy transport at lower levels and southward dry static energy transport at upper levels in the Southern Hemisphere low latitudes reported by Wang et al. (2024). The HC tends to shift toward the warming hemisphere (Northern Hemisphere in this study), which facilitates the release of excess energy in the Northern Hemisphere through convection and enhances southward cross-equatorial energy transport in the upper atmosphere. To maintain interhemispheric energy balance,

the enhanced total atmospheric southward energy transport compensates for the intensified northward oceanic heat transport, primarily driven by the strengthened AMOC resulting from the establishment of the ACC, which is a manifestation of Bjerknes compensation (Bjerknes, 1964; Liu et al., 2015; Yang et al., 2016).

4. Mechanisms

ENSO characteristics are closely tied to the background mean climate of the tropical Pacific (Collins, 2000; Fedorov & Philander, 2001). The changes in heat transport and the HC shown in Figure 2 alter the tropical climate, as reflected in the mean state changes depicted in Figure 3. Figure 3 depicts changes in the climatic mean state between the DPO and DPC experiments. Consistent with previous modeling studies conducted under modern greenhouse gas levels and paleogeography (Toggweiler & Samuels, 1995; Toggweiler & Bjornsson, 2000; Sijp & England, 2004, 2005; Yang et al., 2014; Wang et al., 2024, 2025), the opening of the DP leads to a pronounced cooling in Southern Hemisphere air temperature and SST.

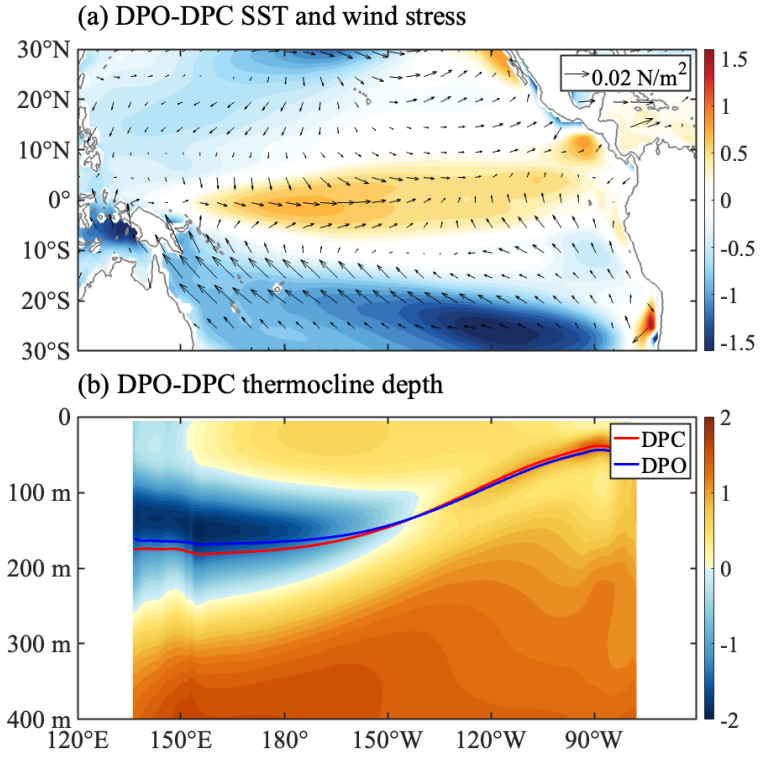

FIG. 3. Changes in Mean Tropical Climate from DPC to DPO: (a) SST (°C) and surface wind stress (N m^{-2}); (b) upper-ocean temperature (°C) averaged between 5°S and 5°N. The red and

black lines represent the mean thermocline depth in DPC and DPO, respectively, defined by the depth of the 20°C isotherm (Fedorov & Philander, 2001).

Consistent with the northward shift and intensification of the lower-level Southern Hemisphere trade winds shown in Figure 2, the trade winds south of 10°S are significantly strengthened in Figure 3a, which leads to warm water accumulation in the equatorial Pacific. This warming is accompanied by an eastward shift of the Pacific convection center, a weakened zonal SST gradient, and strengthened westerly winds over the equatorial central-western Pacific, indicating a weakened Walker circulation (Ashok et al., 2007; Timmermann et al., 2018; Yan et al., 2022, 2025). Due to the spatial pattern of the El Niño-like mean state, the thermocline depth (Fedorov & Philander, 2001) flattens across the equatorial Pacific, shoaling in the west with little change in the east (Figure 3b), which is consistent with the basin-wide warming shown in Figure 3a.

The changes in the mean climate described above, including the El Niño-like mean state, the weakened trade winds near the equator (10°S–0°) (Yang & Zhang, 2008; Yeh et al., 2010; An & Heo, 2019; Wen et al., 2020; Geng et al., 2024), the weakened Walker circulation (Bayr et al., 2020; Trascasa-Castro et al., 2021), and for the subsurface, a flattened thermocline with a reduced vertical temperature gradient (Yeh et al., 2010; Zhao et al., 2021), would typically be expected to reduce ENSO variability. A flatter thermocline is unfavorable for the enhancement of ENSO variability, as it reduces the mean zonal temperature gradient, thereby weakening the strength of the Bjerknes feedback that drives ENSO (Santoso et al., 2011) and reducing the heat content (recharge capacity) of the western Pacific warm pool (Jian et al., 2022). However, ENSO variability nonetheless increases following the opening of the DP (Figure 1).

The patterns of tropical Pacific changes shown in Figure 2 resemble those reported in experiments with the Tibetan Plateau removed, which also enhance ENSO variability (Wen & Yang, 2020; Yang et al., 2020; Wen et al., 2020). Through analysis of the temperature variance equation, Yang and Zhang (2008) and Wen et al. (2020) confirmed that the vertical advection term is the primary contributor to ENSO variability. Wen et al. (2020) found that removal of the Tibetan Plateau shifts both the wind stress response to Niño-3 SST anomalies and the sensitive region of anomalous Ekman upwelling in the equatorial Pacific (Jin et al., 2006) eastward, significantly enhancing temperature variance in the Niño-3 region and thereby intensifying ENSO. In this study, these processes are initiated by topographic changes in the Southern Hemisphere.

Figure 4 shows the total vertical advection term ($-wT'T_z$), its local and remote modes ($-w'T'\overline{T}_z$, $-\overline{w}T'T'_z$), and the variables constituting these terms in the Niño region for the DPC and DPO experiments. Consistent with previous studies, the remote mode acts as a damping effect by transporting water with lower variability from deeper layers upward via mean upwelling, thereby suppressing temperature variability (Figure 4a). The local mode within the vertical advection term is the primary positive contributor to temperature variability in the Niño-3 region, and its enhancement is the main reason for the increase in ENSO variability following the opening of the DP (Yang & Zhang, 2008; Wen et al., 2020). Analysis of the components of the local mode reveals that although the vertical temperature gradient ($\overline{T_z}$) slightly decreases, anomalous upwelling (w') strengthens (Figure 4c). Positive anomalous upwelling represents stronger cold water upwelling, reducing thermocline temperature. Therefore, the vertical heat flux ($-w'T'$) significantly increases in the DPO experiment, which is the primary reason for the enhancement of ENSO variability.

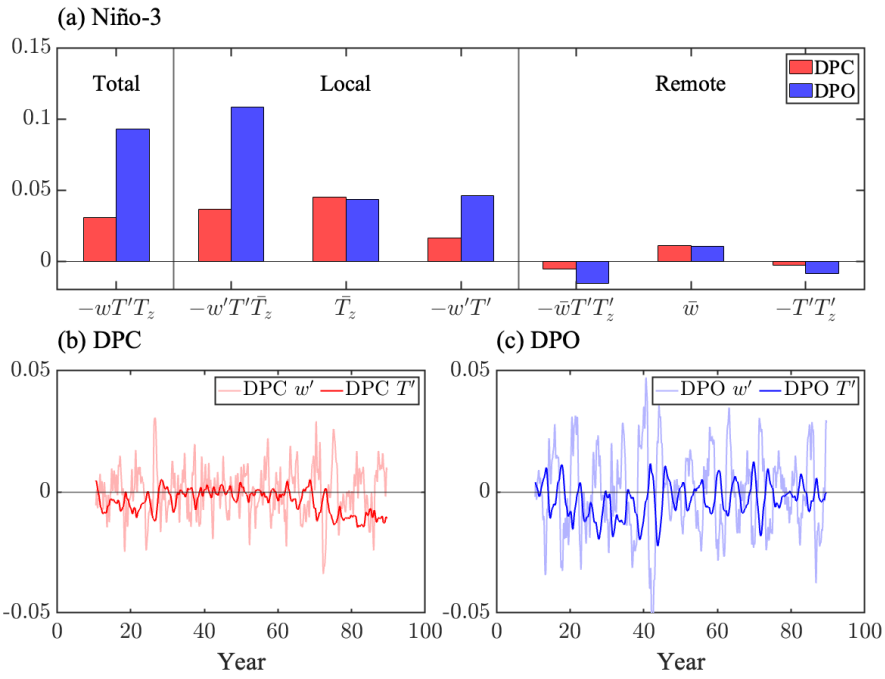

FIG. 4. (a) Mean values of the total, local, and remote terms and their components averaged over the thermocline in the Niño-3 region; (b) and (c) schematic showing anomalous upwelling and temperature anomalies in the Niño-3 region for the DPC and DPO experiments, respectively. Each curve is smoothed with a 21-year running mean. The values of $\overline{w}$, w', $\overline{T_z}$, $w'T'$, $T'T'_z$ and T' are plotted after being multiplied by 2×10^{1}, 10^{4}, 2×10^{-1}, 10^{5}, 5, and 10^{-1}, respectively. The units of these terms are $°C^2\ s^{-1}$.

As noted above, the formation of the ACC reduces southward transport of warm water from the mid- and low-latitude regions, leading to significant warming of the thermocline in the tropical Pacific and the Southern Hemisphere subtropics (Figure 5b). This warming is consistent with the subsurface warming shown in Figure 3b and weakens most of the stratification in the Niño-3 region, which is unfavorable for the enhancement of ENSO variability (Fedorov & Philander, 2001; Yang & Zhang, 2008; Yeh et al., 2010; Zhao et al., 2021). This suggests that the adjusted oceanic processes are unfavorable for the enhancement of ENSO variability.

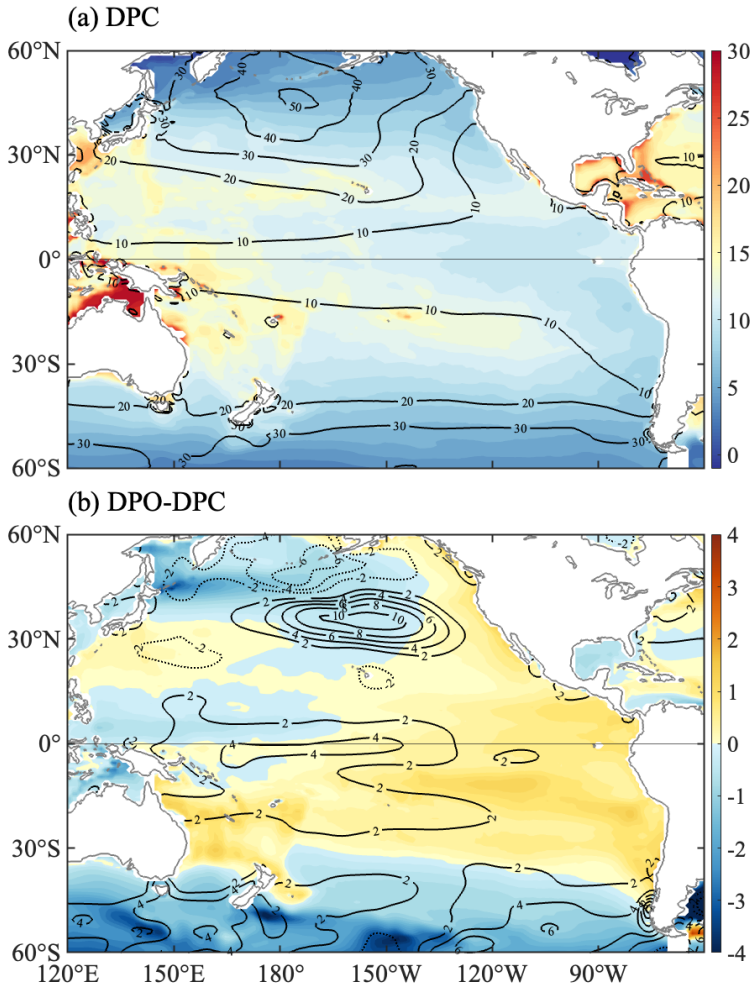

FIG. 5. (a) DPC and (b) DPO minus DPC: contours show zonal wind stress (τ_x) variability (10^{-3} N m^{-2}), with solid lines indicating increased variability and dashed lines indicating decreased variability; shading shows the mean temperature (°C) between 24 and 26 σ, representing thermocline temperature (Yang et al., 2005).

Therefore, the increase in ENSO variability in DPO relative to DPC is attributed to atmospheric changes. The enhanced anomalous upwelling (Figure 4c) results from increased zonal wind stress variability over the central-eastern equatorial Pacific (Figure 5b) (Fedorov & Philander, 2001; Jin et al., 2006; Bayr et al., 2020). Owing to the formation of an El Niño-like mean state, the eastward shift of the convection center, and significant cooling in the Southern Hemisphere (Figure 3a), the increased meridional temperature gradient in this region leads to enhanced wind stress variability (Lindzen & Nigam, 1987). This strengthens anomalous upwelling and the local mode of the vertical advection term in turn, ultimately enhancing ENSO variability (Jin et al., 2006).

5. Conclusions and Discussion

This study employs a fully coupled climate model to investigate the role of the DP opening in ENSO variability. The opening of the DP establishes the ACC and strengthens the AMOC, causing the southern branch of the HC to shift northward and intensify. This triggers a sea surface response in the tropical Pacific characterized by an El Niño-like mean-state climate (Yang & Zhang, 2008; Wen et al., 2020; Geng et al., 2024), manifested as a weakened Walker circulation and a flattened thermocline across the equatorial Pacific. Through analysis of the temperature variance equation, this enhancement is attributed to the strengthening of the local mode within the vertical advection term. Following the DP opening, the increased meridional temperature gradient over the central-eastern equatorial Pacific leads to stronger anomalous zonal wind stress, which in turn enhances anomalous upwelling and vertical heat flux, ultimately resulting in the intensification of the local mode in the vertical advection term.

Both model experiments and paleoclimate proxies indicate that ENSO variability during the Eocene (55–35 Ma), prior to extensive mountain uplift, was greater than in the modern climate (Manabe & Broccoli, 1990; Huber & Caballero, 2003; Kitoh, 2006; Naiman et al., 2017). However, the opening of the DP (~43 Ma) and the establishment of a strong ACC (~32 Ma) also occurred within this interval (Zachos et al., 2001; Lagabrielle et al., 2009). Therefore, the potential impact of the DP opening on enhancing ENSO variability during this period may have been overlooked. By taking this factor into account, our study considers the influence of the evolution of Southern Ocean high-latitude gateway on tropical Pacific climate, which offer valuable insights for understanding the evolution of ENSO since the Eocene.

The opening of the DP is a protracted process (Zachos et al., 2001; Lagabrielle et al., 2009), during which paleogeography and greenhouse gas concentrations underwent substantial changes. Although many details remain unresolved, the opening of the DP has been a key driver in the reorganization of global atmospheric and oceanic circulation and in shaping hemispheric climate changes (Toggweiler & Samuels, 1995; Toggweiler & Bjornsson, 2000; Zachos et al., 2001; Sijp & England, 2004, 2005; Sijp et al., 2009; Lagabrielle et al., 2009; Zhang et al., 2010, 2011; Yang et al., 2014; England et al., 2017; Wang et al., 2024, 2025). The temporal evolution of this event overlaps with the period of rapid global mountain uplift, yet their effects on ENSO variability are opposite (Manabe & Broccoli, 1990; Zachos et al., 2001; Kitoh, 2006; Naiman et al., 2017; Wen et al., 2020). This study identifies this contrast through coupled model experiments. Future work may require additional experiments to investigate the physical processes through which seaway evolution and Southern Ocean climate change influence ENSO variability.

Acknowledgements:

This research is jointly supported by the NSF of China (Nos. 42288101, 42230403 and 41725021) and by the foundation at the Shanghai Frontiers Science Centre of Atmosphere-Ocean Interaction of Fudan University.

Data Availability Statement:

All data and code used in this study are available upon request.

Conflict of interest:

The authors have no relevant financial or non-financial interests to disclose.

REFERENCES

An, S., & Heo, E. S. (2019). Robust opposite-changing tendency between the thermal advection damping by mean current and thermo-dynamical damping of ENSO Feedback in a changing climate. *International Journal of Climatology*, *39*(15), 5822–5829. https://doi.org/10.1002/joc.6176

Ashok, K., Behera, S. K., Rao, S. A., Weng, H., & Yamagata, T. (2007). El Niño Modoki and its possible teleconnection. *Journal of Geophysical Research: Oceans*, *112*, C11007. https://doi.org/10.1029/2006JC003798

Bayr, T., Dommenget, D., & Latif, M. (2020). Walker circulation controls ENSO atmospheric feedbacks in uncoupled and coupled climate model simulations. *Climate Dynamics*, *54*(5–6), 2831–2846. https://doi.org/10.1007/s00382-020-05152-2

Bjerknes, J. (1964). Atlantic Air-Sea Interaction. *Advances in Geophysics*, *10*, 1–82. https://doi.org/10.1016/S0065-2687(08)60005-9

Broccoli, A. J., Dahl, K. A., & Stouffer, R. J. (2006). Response of the ITCZ to Northern Hemisphere cooling. *Geophysical Research Letters*, *33*(1), L01702. https://doi.org/10.1029/2005GL024546

Chen, L., Yu, Y., & Sun, D. (2013). Cloud and water vapor feedbacks to the El Niño warming: Are they still biased in CMIP5 models? *Journal of Climate*, *26*(14), 4947–4961. https://doi.org/10.1175/JCLI-D-12-00575.1

Chidichimo, M. P., Donohue, K. A., Watts, D. R., & Tracey, K. L. (2014). Baroclinic Transport Time Series of the Antarctic Circumpolar Current Measured in Drake Passage. *Journal of Physical Oceanography*, *44*(7), 1829–1853. https://doi.org/10.1175/JPO-D-13-071.1

Cobb, K. M., Charles, C. D., Cheng, H., & Edwards, R. L. (2003). The El Niño–Southern Oscillation and tropical Pacific climate during the last millennium. *Nature*, *424*, 271–276. https://doi.org/10.1038/nature01779

Collins, M. (2000). The El Niño–Southern Oscillation in the second Hadley Centre coupled model and its response to greenhouse warming. *Journal of Climate*, *13*(7), 1299–1312. https://doi.org/10.1175/1520-0442(2000)013<1299:TENOSO>2.0.CO;2

Donohue, K. A., Tracey, K. L., Watts, D. R., Chidichimo, M. P., & Chereskin, T. K. (2016). Mean Antarctic Circumpolar Current transport measured in Drake Passage. *Geophysical Research Letters*, *43*(22), 11760–11767. https://doi.org/10.1002/2016GL070319

England, M. H., Hutchinson, D. K., Santoso, A., & Sijp, W. P. (2017). Ice–Atmosphere Feedbacks Dominate the Response of the Climate System to Drake Passage Closure. *Journal of Climate*, *30*(15), 5775–5790. https://doi.org/10.1175/JCLI-D-15-0554.1

Fallah, B., Cubasch, U., Prommel, K., & Sodoudi, S. (2016). A numerical model study on the behaviour of Asian summer monsoon and AMOC due to orographic forcing of Tibetan Plateau. *Climate Dynamics*, *47*(5), 1485–1495. https://doi.org/10.1007/s00382-015-2914-5

Fedorov, A. V., & Philander, S. G. (2001). A stability analysis of tropical ocean–atmosphere interactions: Bridging measurements and theory for El Niño. *Journal of Climate*, *14*(14), 3086–3101. https://doi.org/10.1175/1520-0442(2001)014<3086:ASAOTO>2.0.CO;2

Feng, R., & Poulsen, C. J. (2014). Andean elevation control on tropical Pacific climate and ENSO. *Paleoceanography*, *29*(8), 795–809. https://doi.org/10.1002/2014PA002640

Geng, T., Cai, W., Jia, F., & Wu, L. (2024). Decreased ENSO post-2100 in response to formation of a permanent El Niño-like state under greenhouse warming. *Nature Communications*, *15*, 5810. https://doi.org/10.1038/s41467-024-50156-9

Guilyardi, E. (2006). El Niño–mean state–seasonal cycle interactions in a multi-model ensemble. *Climate Dynamics*, *26*(4), 329–348. https://doi.org/10.1007/s00382-005-0084-6

Gutierrez-Villanueva, M. O., Chereskin, T. K., & Sprintall, J. (2023). Compensating transport trends in the Drake Passage frontal regions yield no acceleration in net transport. *Nature Communications*, *14*(1), 7792. https://doi.org/10.1038/s41467-023-43499-2

Huber, M., & Caballero, R. (2003). Eocene El Niño: Evidence for Robust Tropical Dynamics in the "Hothouse." *Science*, *299*, 877–881. https://doi.org/10.1126/science.1078766

Hurrell, J. W., Holland, M. M., Gent, P. R., Ghan, S., Kay, J. E., Kushner, P. J., et al. (2013). The community Earth system model: A framework for collaborative research. *Bulletin of the American Meteorological Society*, *94*(9), 1339–1360. https://doi.org/10.1175/BAMS-D-12-00121.1

Jian, Z., Wang, Y., Dang, H., Mohtadi, M., Rosenthal, Y., Lea, D. W., et al. (2022). Warm pool ocean heat content regulates ocean–continent moisture transport. *Nature*, *612*, 92–99. https://doi.org/10.1038/s41586-022-05302-y

Jin, F., Kim, S. T., & Bejarano, L. (2006). A coupled-stability index for ENSO. *Geophysical Research Letters*, *33*(23), L23708. https://doi.org/10.1029/2006GL027221

Kitoh, A. (1997). Mountain uplift and surface temperature changes. *Geophysical Research Letters*, *24*(2), 185–188. https://doi.org/10.1029/96GL03953

Kitoh, A. (2006). ENSO modulation by mountain uplift. *Climate Dynamics*, *28*(7–8), 781–796. https://doi.org/10.1007/s00382-006-0209-6

Kim, S.-Y., Choi, Y.-J., Son, S.-W., Grise, K. M., Staten, P. W., An, S.-I., et al. (2023). Hemispherically asymmetric Hadley cell response to CO2 removal. *Science Advances*, *9*(30), eadg1801. https://doi.org/10.1126/sciadv.adg1801

Koenig, Z., Provost, C., Ferrari, R., Sennéchael, N., & Rio, M. (2014). Volume transport of the Antarctic Circumpolar Current: Production and validation of a 20 year long time series obtained from in situ and satellite observations. *Journal of Geophysical Research: Oceans*, *119*(8), 5407–5433. https://doi.org/10.1002/2014JC009966

Kug, J.-S., Jin, F.-F., & An, S.-I. (2009). Two Types of El Niño Events: Cold Tongue El Niño and Warm Pool El Niño. *Journal of Climate*, *22*(6), 1499–1515. https://doi.org/10.1175/2008JCLI2624.1

Kug, J.-S., Oh, J.-H., An, S.-I., Yeh, S.-W., Min, S.-K., Son, S.-W., et al. (2021). Hysteresis of the intertropical convergence zone to CO2 forcing. *Nature Climate Change*, *12*(1), 47–53. https://doi.org/10.1038/s41558-021-01211-6

Lagabrielle, Y., Goddéris, Y., Donnadieu, Y., Malavieille, J., & Suarez, M. (2009). The tectonic history of Drake Passage and its possible impacts on global climate. *Earth and Planetary Science Letters*, *279*(3–4), 197–211. https://doi.org/10.1016/j.epsl.2008.12.037

Lindzen, R. S., & Nigam, S. (1987). On the Role of Sea Surface Temperature Gradients in Forcing Low-Level Winds and Convergence in the Tropics. *Journal of Atmospheric Sciences*, *44*(17), 2418-2436. https://doi.org/10.1175/1520-0469(1987)044<2418:OTROSS>2.0.CO;2

Liu, W., & Hu, A. (2015). The role of the PMOC in modulating the deglacial shift of the ITCZ. *Climate Dynamics*, *45*(11–12), 3019–3034. https://doi.org/10.1007/s00382-015-2520-6

Liu, Z., & Yang, H. (2003). Extratropical control of tropical climate, the atmospheric bridge and oceanic tunnel. *Geophysical Research Letters*, *30*(5), 1230. https://doi.org/10.1029/2002GL016492

Liu, Z., Lu, Z., Wen, X., Otto-Bliesner, B. L., Timmermann, A., & Cobb, K. M. (2014). Evolution and forcing mechanisms of El Niño over the past 21,000 years. *Nature*, *515*, 550–553. https://doi.org/10.1038/nature13963

Liu, Z., Yang, H., He, C., & Zhao, Y. (2015). A Theory for Bjerknes Compensation: The Role of Climate Feedback. *Journal of Climate*, *29*(1), 191–208. https://doi.org/10.1175/JCLI-D-15-0227.1

Manabe, S., & Broccoli, A. J. (1990). Mountains and Arid Climates of Middle Latitudes. *Science*, *247*, 192–195. https://doi.org/10.1126/science.247.4939.192

McGee, D., Moreno-Chamarro, E., Green, B., Marshall, J., Galbraith, E., & Bradtmiller, L. (2018). Hemispherically asymmetric trade wind changes as signatures of past ITCZ shifts. *Quaternary Science Reviews*, *180*, 214–228. https://doi.org/10.1016/j.quascirev.2017.11.020

McPhaden, M. J., Zebiak, S. E., & Glantz, M. H. (2006). ENSO as an integrating concept in earth science. *Science*, *314*, 1740–1745. https://doi.org/10.1126/science.1132588

Molnar, P., England, P., & Martinod, J. (1993). Mantle dynamics, uplift of the Tibetan Plateau, and the Indian monsoon. *Reviews of Geophysics*, *31*(4), 357–396. https://doi.org/10.1029/93RG02030

Naiman, Z., Goodman, P. J., Krasting, J. P., Malyshev, S. L., Russell, J. L., Stouffer, R. J., & Wittenberg, A. T. (2017). Impact of Mountains on Tropical Circulation in Two Earth System Models. *Journal of Climate*, *30*(11), 4149–4163. https://doi.org/10.1175/JCLI-D-16-0512.1

Oh, J.-H., Kug, J.-S., An, S.-I., Jin, F.-F., McPhaden, M. J., & Shin, J. (2024). Emergent climate change patterns originating from deep ocean warming in climate mitigation scenarios. *Nature Climate Change*, *14*(3), 260–266. https://doi.org/10.1038/s41558-024-01928-0

Rahmstorf, S. (2002). Ocean circulation and climate during the past 120,000 years. *Nature*, *419*, 207–214. https://doi.org/10.1038/nature01090

Ruddiman, W. F., & Kutzbach, J. E. (1989). Forcing of late Cenozoic Northern Hemisphere climate by plateau uplift in southern Asia and the American West. *Journal of Geophysical Research: Atmospheres*, *94*(D15), 18409–18427. https://doi.org/10.1029/JD094iD15p18409

Santoso, A., Cai, W., England, M. H., & Phipps, S. J. (2011). The Role of the Indonesian Throughflow on ENSO Dynamics in a Coupled Climate Model. *Journal of Climate*, *24*(3), 585–601. https://doi.org/10.1175/2010JCLI3745.1

Sijp, W. P., & England, M. H. (2004). Effect of the drake passage throughflow on global climate. *Journal of Physical Oceanography*, *34*(5), 1254–1266. https://doi.org/10.1175/1520-0485(2004)034<1254:EOTDPT>2.0.CO;2

Sijp, W. P., & England, M. H. (2005). Role of the Drake Passage in Controlling the Stability of the Ocean's Thermohaline Circulation. *Journal of Climate*, *18*(12), 1957–1966. https://doi.org/10.1175/JCLI3376.1

Sijp, W. P., England, M. H., & Toggweiler, J. R. (2009). Effect of Ocean Gateway Changes under Greenhouse Warmth. *Journal of Climate*, *22*(24), 6639–6652. https://doi.org/10.1175/2009JCLI3003.1

Song, Y., Li, Y., Forget, G., Hu, A., Li, Q., Shi, J.-R., et al. (2025). Inter-basin contrast in the Southern Ocean warming. *Nature Communications*, *16*, 9063. https://doi.org/10.1038/s41467-025-64112-8

Stouffer, R. J., Yin, J., Gregory, J. M., Dixon, K. W., Spelman, M. J., Hurlin, W., et al. (2006). Investigating the Causes of the Response of the Thermohaline Circulation to Past and Future Climate Changes. *Journal of Climate*, *19*(8), 1365–1387. https://doi.org/10.1175/JCLI3689.1

Sun, D.-Z., Yu, Y., & Zhang, T. (2009). Tropical water vapor and cloud feedbacks in climate models: A further assessment using coupled simulations. *Journal of Climate*, *22*(5), 1287–1304. https://doi.org/10.1175/2008JCLI2267.1

Timmermann, A., An, S.-I., Kug, J.-S., Jin, F.-F., Cai, W., Capotondi, A., et al. (2018). El Niño–Southern Oscillation complexity. *Nature*, *559*, 535–545. https://doi.org/10.1038/s41586-018-0252-6

Toggweiler, J. R., & Samuels, B. (1995). Effect of drake passage on the global thermohaline circulation. *Deep-Sea Research Part I*, *42*(4), 477–500. https://doi.org/10.1016/0967-0637(95)00012-U

Toggweiler, J. R., & Bjornsson, H. (2000). Drake passage and palaeoclimate. *Journal of Quaternary Science*, *15*(4), 319–328. https://doi.org/10.1002/1099-1417(200005)15:4<319::AID-JQS545>3.0.CO;2-C

Tong, M., Yang, H., Jiang, R., & Wu, P. (2025). Pivotal Role of Tibetan Plateau and Antarctic in Shaping Present-Day Atlantic Meridional Overturning Circulation. *Journal of Climate*, *38*(10), 2239–2252. https://doi.org/10.1175/JCLI-D-24-0301.1

Trascasa-Castro, P., Ruprich-Robert, Y., Castruccio, F., & Maycock, A. C. (2021). Warm Phase of AMV Damps ENSO Through Weakened Thermocline Feedback. *Geophysical Research Letters*, *48*(23), e2021GL096149. https://doi.org/10.1029/2021GL096149

Tudhope, A. W., Chilcott, C. P., McCulloch, M. T., Cook, E. R., Chappell, J., Ellam, R. M., et al. (2001). Variability in the El Niño–Southern Oscillation through a glacial–interglacial cycle. *Science*, *291*, 1511–1517. https://doi.org/10.1126/science.1057969

Wang, P., Yang, S., Li, Z., Song, Z., Li, X., & Hu, X. (2024). Role of the Antarctic Circumpolar Circulation in Current Asymmetric Arctic and Antarctic Warming. *Geophysical Research Letters*, *51*(13), e2024GL110265. https://doi.org/10.1029/2024GL110265

Wang, P., Han, Y., Hu, X., Li, Z., Li, X., Fang, Y., Ying, J., & Yang, S. (2025). Impacts of Strengthened Antarctic Circumpolar Current on the Seasonality of Arctic Climate. *Geophysical Research Letters*, *52*(6), e2025GL115211. https://doi.org/10.1029/2025GL115211

Wang, Y.-X., Yang, H.-J., & Furevik, T. (2013). What determines the amplitude of ENSO events? *Atmospheric and Oceanic Science Letters*, *6*(2), 90–96. https://doi.org/10.1080/16742834.2013.11447062

Weaver, A. J., Marotzke, J., Cummins, P. F., & Sarachik, E. S. (1993). Stability and Variability of the Thermohaline Circulation. *Journal of Physical Oceanography*, *23*(1), 39–60. https://doi.org/10.1175/1520-0485(1993)023<0039:SAVOTT>2.0.CO;2

Wen, Q., & Yang, H. (2020). Investigating the Role of the Tibetan Plateau in the Formation of Pacific Meridional Overturning Circulation. *Journal of Climate*, *33*(9), 3603–3617. https://doi.org/10.1175/JCLI-D-19-0206.1

Wen, Q., Doös, K., Lu, Z., Han, Z., & Yang, H. (2020). Investigating the role of the Tibetan Plateau in ENSO variability. *Journal of Climate*, *33*(12), 4835–4852. https://doi.org/10.1175/JCLI-D-19-0422.1

Xie, C., Shi, J., Li, D., Sun, Y., Jiang, J., & Williams, G. D. (2025). Southward shift of the Antarctic Circumpolar Current upstream of Drake Passage maintains a stable circumpolar transport. *Nature Climate Change*, *15*(12), 1324–1332. https://doi.org/10.1038/s41558-025-02478-9

Yan, Z., Wu, B., Li, T., & Tan, G. (2022). Mechanisms Determining Diversity of ENSO-Driven Equatorial Precipitation Anomalies. *Journal of Climate*, *35*(3), 923–939. https://doi.org/10.1175/JCLI-D-21-0363.1

Yan, Z., Wu, B., Li, T., Collins, M., Zhou, T., & Zhou, W. (2025). Increased longitudinal separation of equatorial rainfall responses to Eastern Pacific and Central Pacific El Niño under global warming. *npj Climate and Atmospheric Science*, *8*, 68. https://doi.org/10.1038/s41612-025-00933-0

Yang, H., Zhang, Q., Zhong, Y., Vavrus, S., & Liu, Z. (2005). How does extratropical warming affect ENSO? *Geophysical Research Letters*, *32*(1), L01702. https://doi.org/10.1029/2004GL021624

Yang, H., & Zhang, Q. (2008). Anatomizing the ocean's role in ENSO changes under global warming. *Journal of Climate*, *21*(24), 6539–6555. https://doi.org/10.1175/2008JCLI2324.1

Yang, H., Zhao, Y., & Liu, Z. (2016). Understanding Bjerknes Compensation in Atmosphere and Ocean Heat Transports Using a Coupled Box Model. *Journal of Climate*, *29*(6), 2145–2160. https://doi.org/10.1175/JCLI-D-15-0281.1

Yang, H., Shen, X., Yao, J., & Wen, Q. (2020). Portraying the Impact of the Tibetan Plateau on Global Climate. *Journal of Climate*, *33*(9), 3565–3583. https://doi.org/10.1175/JCLI-D-18-0734.1

Yang, H., Jiang, R., Wen, Q., Liu, Y., Wu, G., & Huang, J. (2024). The role of mountains in shaping the global meridional overturning circulation. *Nature Communications*, *15*, 2602. https://doi.org/10.1038/s41467-024-46856-x

Yang, S., Galbraith, E., & Palter, J. (2014). Coupled climate impacts of the Drake Passage and the Panama Seaway. *Climate Dynamics*, *43*(1–2), 37–52. https://doi.org/10.1007/s00382-013-1809-6

Yeh, S.-W., Dewitte, B., Yim, B. Y., & Noh, Y. (2010). Role of the upper ocean structure in the response of ENSO-like SST variability to global warming. *Climate Dynamics*, *35*(2–3), 355–369. https://doi.org/10.1007/s00382-010-0849-4

Zachos, J., Pagani, M., Sloan, L., Thomas, E., & Billups, K. (2001). Trends, Rhythms, and Aberrations in Global Climate 65 Ma to Present. *Science*, *292*, 686–693. https://doi.org/10.1126/science.1059412

Zhang, Q., Yang, H., Zhong, Y., & Wang, D. (2005). An idealized study of the impact of extratropical climate change on El Niño–Southern Oscillation. *Climate Dynamics*, *25*, 869–880. https://doi.org/10.1007/s00382-005-0062-z

Zhang, Z., Yan, Q., Wang, H. (2010). Has the Drake Passage Played an Essential Role in the Cenozoic Cooling? *Atmospheric and Oceanic Science Letters*, *3*(5), 288–292. https://doi.org/10.1080/16742834.2010.11446884

Zhang, Z., Nisancioglu, K. H., Flatøy, F., Bentsen, M., Bethke, I., and Wang, H. (2011). Tropical seaways played a more important role than high latitude seaways in Cenozoic cooling. *Climate of the Past*, *7*(3), 801–813, https://doi.org/10.5194/cp-7-801-2011

Zhao, S., Jin, F., Long, X., & Cane, M. A. (2021). On the breakdown of ENSO's relationship with thermocline depth in the central-equatorial Pacific. *Geophysical Research Letters*, *48*(9), e2020GL092335. https://doi.org/10.1029/2020GL092335